Paper

Numerical Analysis of Plane Wave Diffraction by a Semi-Infinite Grating

Member Masahiko NISHIMOTO (Kumamoto University)
Member Hiroyoshi IKUNO (Kumamoto University)

Plane wave diffraction by a semi-infinite strip grating is analyzed in order to investigate the end-effect of finite gratings in pure form. In the formulation, the current induced on each strip is divided into periodic current on an infinite strip grating and the correction current induced by the truncation of the periodic structure. These currents are determined by solving a set of integral equations by using the method of moment. Numerical calculations for current distribution, diffraction patterns, and norm of the induced correction currents reveal the end-effects of the semi-infinite grating.

Keywords: semi-infinite grating, finite grating, end-effects, diffraction

1. Introduction

The problem of electromagnetic wave diffraction by gratings has great importance in microwave and optical engineering, and diffraction characteristics of various kinds of gratings have been investigated so far [1]. Most papers have dealt with infinite gratings to which the Floquet theorem is applicable. The actual gratings, however, have finite extent and their diffraction characteristics are different from those of infinite gratings because of the "end-effects" that caused by the ends of the finite gratings. In order to reveal the end-effects, diffraction by finite gratings and related problems have been analyzed, and diffraction characteristics have been investigated [2]-[10]. However, the most suitable model for analyzing the end-effects of finite gratings is a semi-infinite grating, because it can provide end-effects contributions in pure form as the Sommerfeld's solution for half-plane can reveal the mechanisms of edge diffraction. Hills and Karp [11] have analyzed this problem by using the Wiener-Hopf technique and have revealed the interesting diffraction phenomena. In their analysis, the problem have been solved under the assumption that the thin wire elements are widely spaced relative to the wavelength. However, it is necessary to reveal the diffraction characteristics for narrow spacing in using the finite grating for practical applications such as frequency selective surface or polarization selective surface [12]-[13]. In our previous paper [14], we have analyzed the diffraction by a semi-infinite strip grating under the assumption that each strip is narrow relative to the wavelength. That analysis have given us many features of the end-effects of finite gratings, but enough information has not been obtained because the strip width of the actual gratings is not so narrow relative to the wavelength.

In this paper, we numerically analyze the diffraction of plane waves by a semi-infinite strip grating and investigate the end-effects contribution. The method of analysis is based on the method used in [14], but there is no restriction of the strip width and spacing. In the formulation, we divide the current induced on each strip into two currents, the periodic current on the infinite strip grating and the correction current induced by the truncation of the infinite structure. These currents are determined by solving a set of integral equations by using the method of moment. Numerical results for current distribution, diffraction patterns, and radiated powers by the induced currents are shown, and investigate the end-effect contributions.

Throughout this paper, the time factor $e^{-i\omega t}$ is assumed and suppressed.

2. Formulation of the problem

The geometry of the semi-infinite strip grating is shown in Fig.1(a). The spacing between the strips is d and each strip has a width $2a$. The incident wave is an E-polarized plane wave given by

$$E^i(x, y) = e^{-ik(x\sin\theta_i - y\cos\theta_i)} \tag{1}$$

where θ_i is an incident angle, $k=\omega\sqrt{\varepsilon_0\mu_0}=2\pi/\lambda$ is a wavenumber, and λ is a wavelength. The current induced on each strip has only a z-component. For convenience, let us divide the current on the n-th strip $J^h(nd+x)$ $(|x|<a)$ into two parts:

$$J^h(nd+x) = J^p(nd+x) + J^c(nd+x)$$
$$|x| \le a, \qquad n=0,1,2,\cdots \tag{2}$$

where $J^p(nd+x)$ is the current on the infinite strip grating as shown in Fig.1(b) and $J^c(nd+x)$ is the unknown correction current induced by the truncation of the infinite structure. For periodicity of the structure, $J^p(nd+x)$ satisfies the following periodic condition

$$J^p(nd+x) = e^{-in\beta_0 d} J^p(x) \tag{3}$$

$$\beta_0 = k\sin\theta_i \tag{4}$$

From physical consideration, it is obvious that $J^h(nd+x)$ approaches $J^p(nd+x)$ as n increases. Therefore, $J^c(nd+x)$ has a following important property:

$$\| J^c(nd+x) \| \to 0 \qquad \text{as} \quad n\to\infty \tag{5}$$

The integral representations of the scattered field E^P from the infinite strip grating of Fig.1(b) and scattered field E^S

from the semi-infinite grating of Fig.1(a) are expressed as follows:

$$E^p(x, y) = -i\omega\mu_0 \sum_{n=-\infty}^{\infty} e^{-in\beta_0 d}\int_{-a}^{a} J^p(x') \cdot G(x, y\,|\,nd + x', 0)\, dx' \qquad (6)$$

$$E^s(x, y) = -i\omega\mu_0 \sum_{n=0}^{\infty}\int_{-a}^{a} J^h(nd + x') \cdot G(x, y\,|\,nd + x', 0)\, dx' \qquad (7)$$

where $G(x,y|x',y')$ is the two-dimensional Green's function

$$G(x, y\,|\,x', y') = \frac{1}{4i} H_0^{(2)}\left(k\sqrt{(x-x')^2 + (y-y')^2}\right) \qquad (8)$$

and $H_0^{(2)}$ is the Hankel function of the second kind. By applying the boundary condition

$$E^i(nd + x, 0) + E^p(nd + x, 0) = 0$$
$$|x| \le a, \quad n = 0, \pm1, \pm2, \cdots \qquad (9)$$

to Eqs.(6) and (7), and taking into account Eqs.(2) and (3), we can derive the following integral equations for $J^p(x)$ and $J^c(nd+x)$.

$$E^i(x, 0) = i\omega\mu_0 \sum_{n=-\infty}^{\infty} e^{-in\beta_0 d}\int_{-a}^{a} J^p(x') \cdot G(x, 0\,|\,nd + x', 0)\, dx', \quad |x| \le a \qquad (10)$$

$$E^i(md + x, 0) = i\omega\mu_0 \sum_{n=0}^{\infty} e^{-in\beta_0 d}\int_{-a}^{a} J^p(x') \cdot G(md + x, 0\,|\,nd + x', 0)\, dx' + i\omega\mu_0 \sum_{n=0}^{\infty}\int_{-a}^{a} J^c(nd + x') \cdot G(md + x, 0\,|\,nd + x', 0)\, dx'$$
$$|x| \le a, \quad m = 0, 1, 2, \cdots \qquad (11)$$

If $J^p(x)$ is obtained by solving Eq.(10), then $J^c(nd+x)$ can be determined by solving Eq.(11).

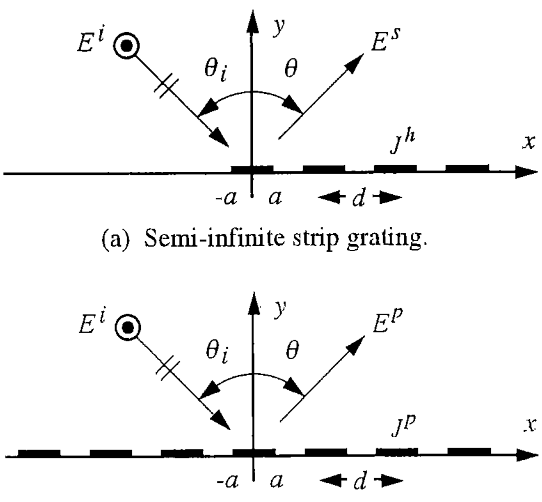

Fig.1 Semi-infinite and infinite strip gratings.

3. Application of the method of moment

In order to solve Eqs.(10) and (11), we use the method of moment (MoM). As the bases function, we employ the pulse function defined by

$$\varphi(x) = \begin{cases} 1 : & 0 \le x \le \Delta\,(= 2a/Q) \\ 0 : & \text{otherwise} \end{cases} \qquad (12)$$

where $\Delta = 2a/Q$ is the pulse width, and Q is the number of discretization of the current. First, we express the unknown current $J^p(x)$ and $J^c(nd+x)$ in terms of $\varphi(x)$ as follows:

$$J^p(x) \approx \sum_{p=0}^{Q-1} A_p \varphi(x + a - p\Delta) \qquad (13)$$

$$J^c(nd + x) \approx \sum_{p=0}^{Q-1} B_{n,p}\varphi(x + a - p\Delta), \quad n = 0, 1, 2, \cdots \qquad (14)$$

where A_p and $B_{n,p}$ are unknown expansion coefficients to be determined. Since the correction current J^c has the property of Eq.(5), coefficients $B_{n,p}$ have following property.

$$|B_{n,p}| \to 0 \quad \text{as } n \to \infty \quad (p = 0, 1, 2, \cdots, Q-1) \qquad (15)$$

As the weighting function, we employ the delta function $\delta(x+a-(q+1/2)\Delta)$ $(q = 0, 1, 2, \dots, Q-1)$ (point matching). The procedure of standard MoM leads to the following simultaneous equations to determine the unknown coefficients A_p and $B_{n,p}$ as follows:

$$\sum_{p=0}^{Q-1} A_p \left[\sum_{n=-\infty}^{\infty} e^{-in\beta_0 d} G_{n,p-q} \right] = \frac{1}{i\omega\mu_0 \Delta} E^i_{0,q}$$
$$q = 0, 1, 2, \cdots, Q-1 \qquad (16)$$

$$\sum_{n=0}^{\infty}\sum_{p=0}^{Q-1} B_{n,p} G_{n-m,p-q} = \frac{1}{i\omega\mu_0\Delta} E^i_{m,q} - \sum_{p=0}^{Q-1} A_p \left[\sum_{n=0}^{\infty} e^{-in\beta_0 d} G_{n-m,p-q} \right] \qquad (17)$$
$$q = 0, 1, 2, \cdots, Q-1, \quad m = 0, 1, 2, \cdots$$

where

$$G_{n,p} \simeq \begin{cases} \dfrac{1}{4i} H_0^{(2)}(k\,|nd + p\Delta|) & : n \ne 0 \text{ or } p \ne 0 \\ \dfrac{1}{4i}\left[1 + \dfrac{2i}{\pi}(1-\gamma) - \dfrac{2i}{\pi}\ln\dfrac{k\Delta}{4} + \left(\dfrac{1}{48} - \dfrac{i\gamma}{24\pi} + \dfrac{i}{18\pi} + \dfrac{i}{24\pi}\ln\dfrac{k\Delta}{4}\right)(k\Delta)^2 \right] & : n = p = 0 \end{cases} \qquad (18)$$

$$E^i_{m,q} = \int_{-a}^{a} E^i(md + x, 0)\,\delta(x + a - (q + 1/2)\Delta)\, dx = e^{-i\beta_0(md - a + (q+1/2)\Delta)} \qquad (19)$$

and $\gamma = 0.5772 \dots$ is Euler's constant. In the calculation of $G_{n,p}$, we have taken into account that the pulse width Δ is sufficiently small relative to the wavelength, and have used the approximation of the Hankel function for small argument. From Eq.(16) the unknown coefficients A_p are determined. Once the A_p are known, other coefficients $B_{n,p}$ are determined from Eq.(17). Although Eq.(17) is an infinite dimensional simultaneous equations, we can truncate it and solve it numerically, because $B_{n,p}$ approaches zero as n increases (see Eq.(15)).

4. Scattered field

Taking account of Eq.(2), scattered field of Eq.(7) is expressed as follows:

$$E^s(x, y) = E^{s(p)}(x, y) + E^{s(c)}(x, y) \tag{20}$$

where $E^{s(p)}$ and $E^{s(c)}$ are the fields radiated by the currents J^p and J^c respectively. Scattered field $E^{s(p)}$, in which the effect of the correction currents is not include, is called a "Kirchhoff solution" [11]. Substituting Eqs.(2) and (3) into Eq.(7), and transforming the spatial integral into spectrum domain, we have following spectral integral representations.

$$E^{s(p)}(x, y) = -\frac{\omega\mu_0\Delta}{4\pi}\sum_{p=0}^{Q-1} A_p \cdot \int_C \frac{F_p(\zeta)\, e^{\mp iy\sqrt{k^2-\zeta^2}}\, e^{-i\zeta x}}{\sqrt{k^2-\zeta^2}\left(1-e^{-i(\beta_0-\zeta)d}\right)}\, d\zeta, \quad (y \lessgtr 0) \tag{21}$$

$$E^{s(c)}(x, y) = -\frac{\omega\mu_0\Delta}{4\pi}\sum_{n=0}^{\infty}\sum_{p=0}^{Q-1} B_{n,p} \cdot \int_C \frac{F_p(\zeta)\, e^{\mp iy\sqrt{k^2-\zeta^2}-i(x-nd)\zeta}}{\sqrt{k^2-\zeta^2}}\, d\zeta, \quad (y \lessgtr 0) \tag{22}$$

where

$$F_p(\zeta) = \frac{\sin(\zeta\Delta/2)}{\zeta\Delta/2}\, e^{i(-a+(p+1/2)\Delta)\zeta} \tag{23}$$

and branch of $\sqrt{k^2-\zeta^2}$ is as follows:

$$\sqrt{k^2-\zeta^2} = \begin{cases} \sqrt{k^2-\zeta^2} & : k > |\zeta| \\ -i\sqrt{\zeta^2-k^2} & : k < |\zeta| \end{cases} \tag{24}$$

The contour C is the infinite path in the ζ plane as shown in Fig.2, where it is assumed that k has a small negative imaginary part. The poles of Eq.(21) located at $\zeta = \beta_m = \beta_0 + 2m\pi/d$ correspond to the Floquet's modes of the infinite grating.

Next, in order to derive the far field representation, we evaluate the integrals of Eqs.(21) and (22) for $kr = k\sqrt{x^2+y^2} \gg 1$ by using the saddle point method.

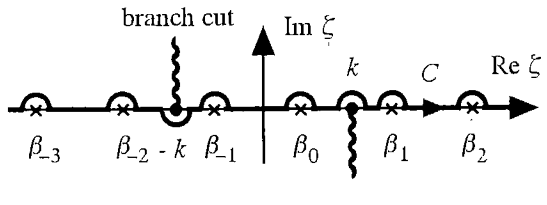

Fig.2 Contour C in complex ζ plane.

Since the scattered field E^s is symmetric with respect to x-axis, we shall derive the far field representation for $|\theta| \le \pi/2$. Let us introduce the following change of variables.

$$\zeta = k\sin w, \quad x = r\sin\theta, \quad y = r\cos\theta. \tag{25}$$

Substituting Eq.(25) into Eqs.(21) and (22), and evaluating the integrals by the saddle point method [15], we can obtain the uniform asymptotic expression as follows:

$$E^s(r, \theta) = E^g(r, \theta) + E^d(r, \theta) \tag{26}$$

where

$$E^g(r, \theta) = -\frac{\omega\mu_0\Delta}{2d}\sum_{p=0}^{Q-1} A_p \sum_{m=-\infty}^{\infty} \frac{F_p(\beta_m)}{\sqrt{k^2-\beta_m^2}} \cdot e^{-ikr\cos(\theta-w_m^p)}\, u(\theta-w_m^p) \tag{27}$$

$$\begin{aligned} E^d(r, \theta) = &-\frac{\omega\mu_0\Delta}{2d}\sum_{p=0}^{Q-1} A_p \sum_{m=-\infty}^{\infty}\Big[-\mathrm{sgn}(\theta-w_m^p) \frac{F_p(\beta_m)}{\sqrt{k^2-\beta_m^2}}\, e^{-ikr\cos(\theta-w_m^p)}\, \frac{e^{-i\pi/4}}{\sqrt{\pi}}\Phi(\zeta_m)\Big] \\ &-\frac{\omega\mu_0\Delta}{4}\sqrt{\frac{2}{\pi kr}}\, e^{-i(kr-\pi/4)} \cdot \sum_{p=0}^{Q-1}\Big[A_p\Big\{\frac{F_p(k\sin\theta)}{1-\exp[-ikd(\sin\theta_i-\sin\theta)]} \\ &-\frac{i}{2d}\sum_{m=-\infty}^{\infty}\frac{F_p(\beta_m)}{\sqrt{k^2-\beta_m^2}}\,\frac{1}{\sin\left((\theta-w_m^p)/2\right)}\Big\} \\ &+F_p(k\sin\theta)\sum_{n=0}^{\infty} B_{n,p}\, e^{inkd\sin\theta}\Big] \end{aligned} \tag{28}$$

$$\zeta_m = \sqrt{2kr}\,\sin(|\theta-w_m^p|/2) \tag{29}$$

$$\Phi(\xi) = \int_{\xi}^{\infty} e^{-it^2}\, dt \tag{30}$$

$$u(\theta) = \begin{cases} 1 : \theta > 0 \\ 0 : \theta < 0 \end{cases} \tag{31}$$

and $w_m^p = \arcsin(\beta_m/k)$, which are the poles of Eq.(21), correspond to the Floquet's modes of periodic structure. Eq.(26) indicates that the scattered field by a semi-infinite grating is expressed as a sum of two types of waves, E^g and E^d. The wave E^g, which is the residue contribution of Eq.(21), is a set of plane waves (Floquet waves) and E^d is a diffracted wave at the end of the semi-infinite grating. It can be shown that the amplitudes and the directions of propagation of the plane waves of E^g coincide with those of Floquet waves of the infinite grating shown in Fig.1(b). It is, however, found from Eq.(27) that they exist only within the region $w_m^p < \theta \le \pi/2$. Thus, the lines $\theta = w_m^p$ act as the shadow or reflection boundaries of the Floquet waves similar to those appearing in the diffraction by a conducting half plane. This result is also pointed out by Hills and Karp [11]. The first term of Eq.(28), which is derived form Eq.(21), is a contribution of higher order term of uniform asymptotic evaluation when the poles and saddle point close to each other. This term removes the singularities of the diffracted field in the transition regions

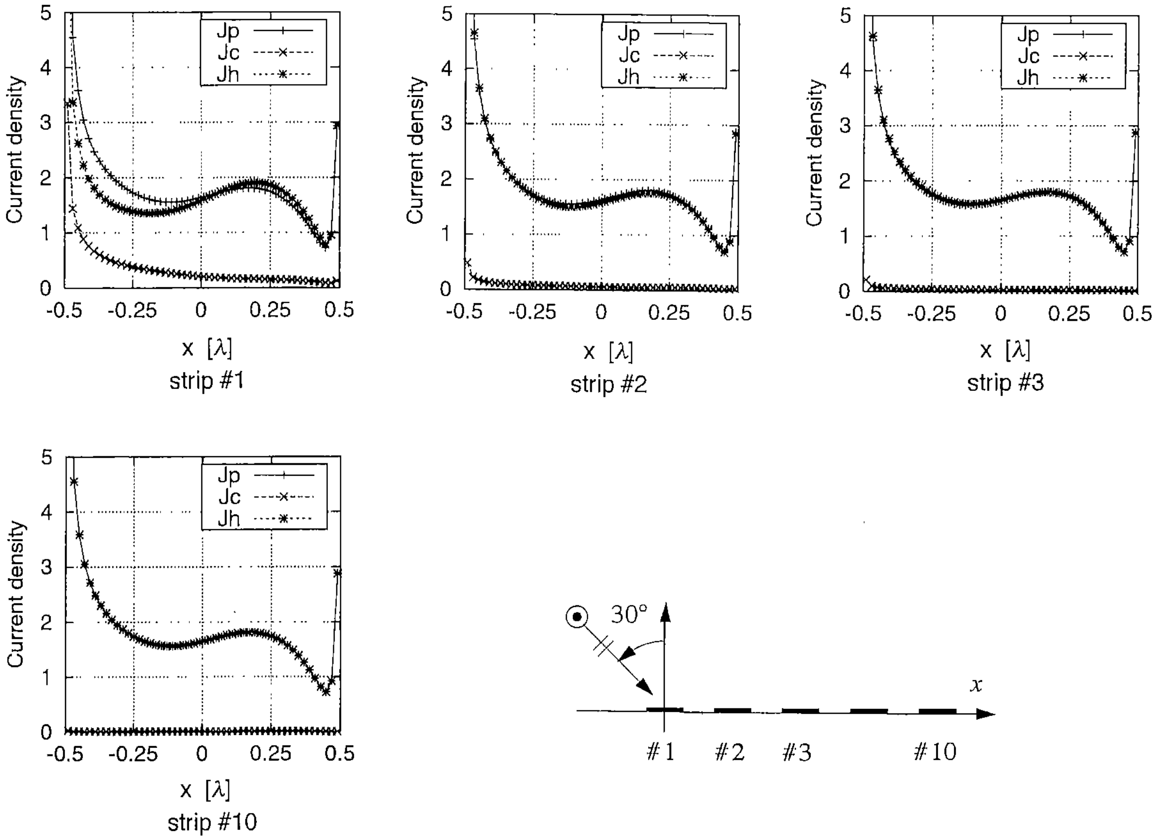

Fig. 3. Current distributions on the strip #1, #2, #3, and #10. ($2a = 1\lambda,\ d = 1.5\lambda,\ \theta_i = 30°$)

near shadow and reflection boundaries where the first order solution of saddle point method fails. The second term of Eq.(28), which is derived form Eqs.(21) and (22), is a cylindrical wave diffracted at the end of the grating.

5. Numerical results and discussions

Numerical calculations are carried out for current distributions on the strip elements located near the edge, diffraction and scattering patterns, and norm of the correction currents that is defined for the quantitative evaluation of the end- effect. In order to obtain accurate solutions, the choice of the pulse width Δ becomes important. In reference [16], it is shown that, for scattering by single strip, $\Delta = \lambda/50$ is sufficiently small to get an accurate solution (energy error is less than 1%). According to this fact, we shall chose the width of the pulse as $\Delta = \lambda/50$.

Figure 3 shows the current distributions on the strip #1, #2, #3, and #10. This figure indicates that the correction current J^c on the edge strip (#1) is comparatively large and it becomes small as the strip number increases. On the strip #10 that is located far away from the edge, J^c, as we expected, becomes negligibly small and total current J^h coincides with periodic current J^p on the infinite grating. In order to evaluate the behavior of the correction currents, we also calculate the norm of the correction currents defined by

$$J_n^c = \sqrt{\int_{-a}^{a} \left| J^c(nd + x) \right|^2 dx} \ . \qquad (32)$$

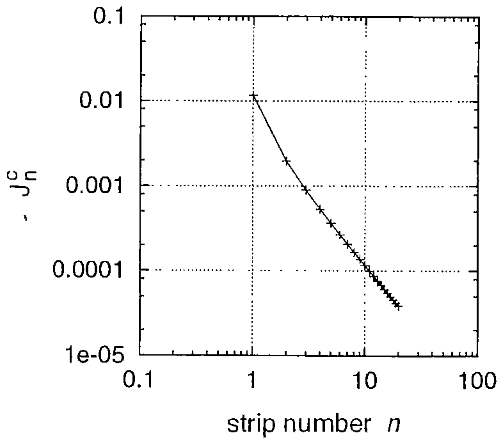

Fig. 4. Norm of the correction current J_n^c on each strip. ($2a = 1\lambda,\ d = 1.5\lambda,\ \theta_i = 30°$)

Figure 4 shows the log scale representation of the norm of the correction current on each strip. From this result, we can confirm that correction currents act $J_n^c \propto n^{-3/2}$ as the strip number increases, and Eq.(5) is satisfied.

Figure 5 shows the diffraction pattern E^d given by Eq.(27) for the same parameters of Fig.3. The pattern is normalized by one half of the intensity of the incident wave. The Kirchhoff solution, which are obtained by letting $J^c = 0$, are also shown by the broken line. It is found from this result that the diffraction at 90° and -38° is

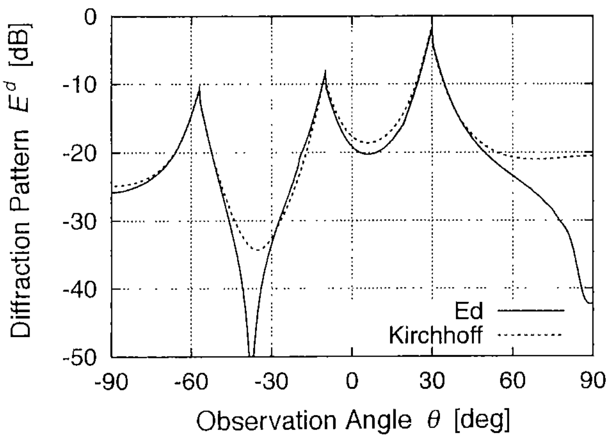

Fig. 5. Diffraction pattern E^d.
($2a = 1\lambda,\ d = 1.5\lambda,\ \theta_i = 30°,\ kr = 50\lambda,$)

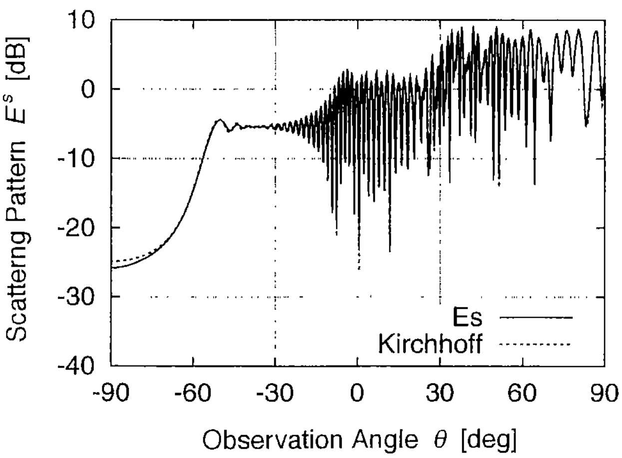

Fig. 6. Scattering pattern E^S.
($2a = 1\lambda,\ d = 1.5\lambda,\ \theta_i = 30°,\ kr = 50\lambda,$)

suppressed by the effect of the correction currents. When the width of the strip is narrow ($2a << \lambda$), we have pointed out that the diffraction pattern has sharp nulls in some directions [14]. However, this result indicates that those nulls do not appear except for at $\theta = 90°$ and -38° when the width of the strip is not narrow. For this configuration ($d = 1.5\lambda,\ \theta_i = 30°$), reflection boundaries of the 0-th, -1st, and -2nd order Floquet waves appear in the directions θ = 30°, -9.6°, and -56.5°, respectively. In the diffraction pattern, we can observe discontinuities in these directions. On the other hand, Fig. 6 shows the scattering pattern E^s that is given by Eq.(26). Since the Floquet waves E^g is added to the field, the discontinuities of the pattern disappear. In the regions $-9.6° < \theta < 30°$ and $30° < \theta < 90°$, we can find the oscillation of the pattern caused by the interference of the Floquet waves.

Next, we shall quantitatively evaluate the end-effects contribution. Since the end-effect of the semi-infinite gratings is considered as the effects caused by the correction current J^c, we calculate the total norm of the correction currents in order to estimate the degree of the

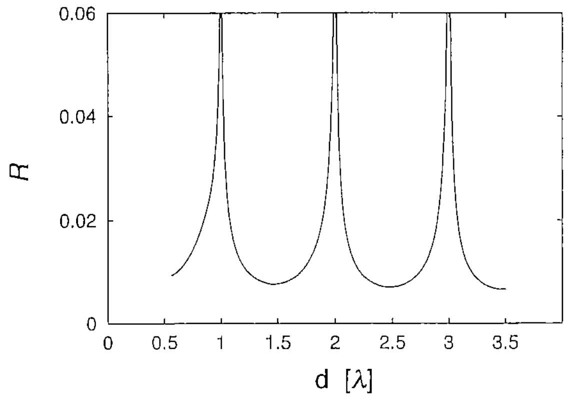

Fig. 7. End-effect R versus spacing d.
($2a = 0.5\lambda,\ \theta_i = 0°$)

end-effects contribution. The total norm R is defined by

$$R = \sum_{n=1}^{\infty} \left\| J^c(nd + x) \right\|^2 = \sum_{n=1}^{\infty} \int_{-a}^{a} \left| J^c(nd + x) \right|^2 dx \qquad (33)$$

Figure 7 shows the total norm R versus the spacing d. We can find, from this figure, that R becomes large when $d = m\lambda$ for $\theta_i = 0°$ where $m = 1,2,3,\ldots$. For infinite grating, these values correspond to the spacing for cut-off of the m-th mode, and the multiple scattering between the elements becomes strong (or the Wood's type anomaly occurs). Therefore, this result indicates that the end-effect of the semi-infinite grating becomes large for cut-off frequencies of Floquet waves.

6. Conclusions

In this paper, we have numerically analyzed the plane wave diffraction by a semi-infinite strip grating and have investigated the end-effects contribution in pure form. Numerical results of current distributions and diffraction pattern have revealed the behavior of the currents near the edge and diffraction properties. It has also been revealed that the end-effect contribution becomes large for cutoff frequencies of the Floquet waves. These results are very useful for evaluating the diffraction by finite gratings. Furthermore, according to the concept of the GTD, we can easily derive the diffraction coefficients of semi-infinite grating, and will be able to use them in calculating the diffraction by a very large finite grating.

In order to investigate the end-effect contribution in more detail, we have to calculate the near field around the edge. This analysis is left as future problem.

(Manuscript received January 30, 2001, revised May 30, 2001)

References

[1] R. Petit Ed., "Electromagnetic theory of gratings", Series topics in current physics, Springer-Verlag, New York, 1980.

[2] V. Twelsky, "On a multiple scattering theory of the finite grating and Wood's anomalies", *J. Appl. Phys.*, vol. 23, No.10, pp.1099-1118, 1952.
[3] W.L. Ko and R. Mittra, "Scattering by a truncated periodic array", *IEEE Trans. Antennas & Propagat.*, vol. AP-36, No.4, pp.496-503, 1988.
[4] K. Kobayashi and T. Eizawa, "Plane wave diffraction by a finite sinusoidal grating", *Trans. IEICE*, vol. E74, No.9, pp.2815-2826, 1991.
[5] L. Carin and L.B. Felsen, "Time-harmonic and transient scattering by finite periodic flat strip arrays: Hybrid (Ray)-(Floquet's Mode)-(MOM) algorithm and its GTD interpretation", *IEEE Trans. Antennas & Propagat.*, vol. AP-41, No.4, pp.412-421, 1993.
[6] L.B. Felsen and L. Carin, "Diffraction theory of frequency- and time-domain scattering by weakly aperiodic truncated thin-wire gratings", *J. Opt. Soc. Amer.*, vol. 11, No.4, pp.1291-1306, 1994.
[7] J. M. Usoff and B. A. Munk, "Edge effects of truncated periodic surfaces of thin wire elements", *IEEE Trans. Antennas & Propagat.*, vol. AP-42, No.7, pp.946-953, 1994.
[8] F. Capolino, M. Albani, S. Maci, and L. B. Felsen, "Frequency domain Green's function for a planar periodic semi-infinite phased array. Part I and II", *IEEE Trans. Antennas & Propagat.*, vol. AP-48, No.1, pp.67-85, 2000.
[9] A. Neto, S. Maci, G. Vecchi, and M. Sabbadini, "A truncated Floquet wave diffraction method for the full wave analysis of large phased arrays - Part I and Part II", *IEEE Trans. Antennas & Propagat.*, vol. AP-48, No.3, pp.594-611, 2000.
[10] J. Nakayama, "Periodic Fourier transform and its application to wave scattering from a finite periodic surface", *IEICE Trans. Electronics*, vol. E83, No.3, pp.481-487, 2000.
[11] N.L. Hills and S.N. Karp, "Semi-infinite diffraction gratings I and II", *Commu. Pure Appl. Math.*, vol. 18, pp.203-233, pp.389-398, 1965.
[12] R. Mittra, C.H.Chan, and T. Cwik, "Techniques for analyzing frequency selective surfaces - A Review", *Proc. IEEE*, vol. 76, No.12, pp.1593-1615, 1988.
[13] M. Ando and K. Takei, "Reflection and transmission coefficients of a thin strip grating for antenna application", *IEEE Trans. Antennas & Propagat.*, vol. AP-35, No.4, pp.367-3 71, 1987.
[14] M. Nishimoto and H.Ikuno, "Analysis of electromagnetic wave diffraction by a semi-infinite strip grating and evaluation of end-effects", Progress In Electromagnetic Research (PIER), vol.23, pp.39-57, 1999.
[15] L.B.Felsen and N.Marcuvits, "Radiation and scattering of waves", Chap.4, Prentice-Hall, 1973.
[16] A. Matsushima and T. Itakura, "Singular integral equation approach to electromagnetic scattering from a finite periodic array of conducting strips", *J. Electromagnetic Wave and Applications*, vol. 5, No.6, pp.545-562, 1991.

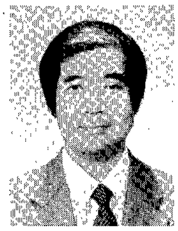

Masahiko Nishimoto (Member) received the B.S. degree in Electronic Engineering from Kumamoto University, Japan, in 1982, and M.S. and D.E. degree in Computer Science and Communication Engineering, from Kyushu University, Fukuoka, Japan, in 1984 and 1987, respectively. Since 1987 he has been with a department of Electrical Engineering and Computer Science, Kumamoto University, where he is currently an Associate Professor. His research interests are in the area of scattering and diffraction of electromagnetic waves, especially high-frequency analysis and time-frequency analysis. Dr. Nishimoto is a member of IEEE and IEICE.

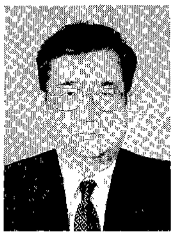

Hiroyoshi Ikuno (Member) received the B.E., M.E., and D.E. degrees in Computer Science and Communication Engineering, from Kyushu University, Fukuoka, Japan, in 1962, 1964, and 1979, respectively. From 1967 to 1970 he was a Research Associate of Computer Science and Communication Engineering at Kyushu University. He joined the Department of Electrical Engineering and Computer Science of Kumamoto University, Kumamoto, Japan, in 1970, and is currently a Professor. During 1983 to 1984, he was a Visiting Professor at Polytechnic University, Brooklyn, NY. From 1997, he is the Chairman of the Technical Group on Electromagnetic Theory in IEE of Japan and IEICE. His research interests are in the area of scattering, diffraction, geometrical optics, wave propagation in the optical waveguide, and computational electromagnetics. Dr. Ikuno is a Senior member of IEEE and member of IEICE.